iEnergy
LETTER
https://doi.org/10.23919/IEN.2024.0015

Resilience-assuring hydrogen-powered microgrids

Chaofan Lin[1], Peng Zhang[1] ✉, Yacov A. Shamash[1], Zongli Lin[2] and Xiaonan Lu[3]

ABSTRACT

Green hydrogen has shown great potential to power microgrids as a primary source, whereas the resilient operation methodology under extreme events remains an open area. To fill this gap, this letter establishes an operational optimization strategy towards resilient hydrogen-powered microgrids. The frequency and voltage regulation characteristics of primary hydrogen sources under droop control and their electrical-chemical conversion process with nonlinear stack efficiency are accurately modeled by piecewise linear constraints. A resilience-oriented multi-time-slot stochastic optimization model is then formulated for an economic and robust operation under changing uncertainties. Test results show that the new formulation can leverage the primary hydrogen sources to achieve a resilience and safety-assured operation plan, supplying maximum critical loads while significantly reducing the frequency and voltage variations.

KEYWORDS

Microgrid operation, resilience, hydrogen, optimization, control.

Increasingly frequent natural disasters and cyber/physical attacks pose an urgent need to build resilient microgrids in communities[1]. Clean hydrogen provides an opportunity to increase microgrid resilience while reducing carbon emission[2]. Although there exist off-the-shelf models for optimal operation of microgrids[3], the hydrogen sources have not yet been taken as the primary source to support microgrid operation. Further, a more accurate model of hydrogen sources, that includes the frequency and voltage regulation characteristics and the nonlinear stack efficiency[4, 5], is needed in the optimization so as to ensure a resilient operation of microgrids under disturbances. Thus, this letter formulates a new resilience-oriented stochastic optimization with accurately modeled hydrogen operational constraints, and provides key insights on how primary hydrogen sources could contribute to the system resilience under extreme events.

1 Problem statement

The hydrogen-based sources equipped with droop control are able to provide frequency and voltage regulations and maintain stable operations of microgrids[4]. For this reason, hydrogen-powered microgrids are able to maintain continuous power supply to the critical loads therein upon the occurrence of blackouts. To quantify the system resilience, a three-stage method[6] is generally used to reflect the overall performance before, during, and after events from a planning perspective. However, since this letter focuses on operation, the resilience metric is defined by the short-term load served ratio (LSR) at each time slot[1]:

$$LSR(\boldsymbol{\lambda}, t) = \sum_{i\in \boldsymbol{N}} \lambda_{i,t} P_{i,t}^{\text{Lreal}} \Big/ \sum_{i\in \boldsymbol{N}} P_{i,t}^{\text{Lreal}} \tag{1}$$

where $\boldsymbol{N}$ is the set of buses; $\boldsymbol{\lambda} = (\lambda_{1,t}, \lambda_{2,t}, ..., \lambda_{N,t})^{\text{T}}$ where $\lambda_{i,t}$ is the binary variable to decide whether to serve the load at bus i or not at time t and N is the number of buses; $P_{i,t}^{\text{Lreal}}$ is the real measured active power of the load.

To be used in extreme conditions, the optimization model in this letter assumes: (1) The microgrid is disconnected from the main grid; (2) The states of all components, including the primary hydrogen sources and other secondary sources, branches, etc., are known and only those in good condition are taken into account; (3) The communication system is down and thus the automatic secondary and tertiary control of distributed energy resources (DERs) are invalid; (4) Manually adjusting the references of DERs and connections of loads is available but needs time; (5) The time-series curves for renewable power outputs and load demands within the optimization time window can be forecast with some errors, while the specific forecast method is beyond this letter's focus.

2 Optimization formulation

The objective of the resilient operation of microgrids is to maximize the weighted served loads under uncertain scenarios[1]:

$$obj = \max \sum_{s\in \boldsymbol{S}} \eta_s \sum_{t\in \boldsymbol{T}} \sum_{i\in \boldsymbol{N}} \lambda_{i,t} w_i P_{s,i,t}^{\text{L}} \tag{2}$$

where $\boldsymbol{S}$ is the set of uncertain scenarios of renewable power outputs and load demands which can be generated by adding the samples of forecast error to the forecast time-series power curve; η_s is the weight of scenario s; $\boldsymbol{T}$ is the set of decision time-slots; w_i is the weight of the load at bus i; $P_{s,i,t}^{\text{L}}$ is the active power of the load at time t and scenario s.

The hydrogen constraints, as the major contribution of this letter, are categorized into two types and elaborated as follows.

• Type 1: Frequency and voltage regulation constraints

For frequency regulation, considering the separate electrolyzer and fuel cell structure of hydrogen sources, as well as their active power limits, the $f-P$ characteristic under droop control can be formulated as follows:

$$P_{s,i,t}^{\text{He}} = \begin{cases} P_i^{\text{HeM}}, f_{s,t} \geqslant f_{i,t}^{\text{HeM}} \\ P_i^{\text{HeM}} - D_i^{\text{HeP}}(f_{i,t}^{\text{HeM}} - f_{s,t}), \text{ others}, \ i \in \boldsymbol{N}_{\text{H}} \\ 0, P_i^{\text{HeM}} - D_i^{\text{HeP}}(f_{i,t}^{\text{HeM}} - f_{s,t}) \leqslant 0 \end{cases} \tag{3}$$

[1]Department of Electrical and Computer Engineering, Stony Brook University, Stony Brook, NY 11794, USA; [2]Department of Electrical and Computer Engineering, University of Virginia, Charlottesville, VA 22904, USA; [3]School of Engineering Technology, Purdue University, West Lafayette, IN 47906, USA
Address correspondence to Peng Zhang, p.zhang@stonybrook.edu

$$P_{s,i,t}^{\mathrm{Hf}}=\begin{cases}P_i^{\mathrm{HfM}}, f_{s,t}\leqslant f_{i,t}^{\mathrm{HfM}}\\ P_i^{\mathrm{HfM}}-D_i^{\mathrm{HfP}}(f_{s,t}-f_{i,t}^{\mathrm{HfM}}),\ \text{others},\ i\in\boldsymbol{N}_{\mathrm{H}}\\ 0, P_i^{\mathrm{HfM}}-D_i^{\mathrm{HfP}}(f_{s,t}-f_{i,t}^{\mathrm{HfM}})\leqslant 0\end{cases}\tag{4}$$

where $\boldsymbol{N}_{\mathrm{H}}$ is the set of buses with hydrogen integration; $P_{s,i,t}^{\mathrm{He}}$ and $P_{s,i,t}^{\mathrm{Hf}}$ are the active power input and output of the electrolyzer and fuel cell; P_i^{HeM} and P_i^{HfM} are the maximum input and output; $f_{i,t}^{\mathrm{HeM}}$ and $f_{i,t}^{\mathrm{HfM}}$ are the droop mode thresholds; D_i^{HeP} and D_i^{HfP} are the droop coefficients.

For voltage regulation, either electrolyzer or fuel cell can provide droop support within their reactive power limits. A dead band is usually set between reactive power generation and absorption[7]. Thus, the $U-Q$ characteristic for hydrogen sources under droop control can be formulated as

$$Q_{s,i,t}^{\mathrm{H}}=\begin{cases}Q_i^{\mathrm{GM}}, D_i^{\mathrm{GQ}}(U_{i,t}^{\mathrm{GM}}-U_{s,i,t})>Q_i^{\mathrm{GM}}\\ D_i^{\mathrm{GQ}}(U_{i,t}^{\mathrm{GM}}-U_{s,i,t}), U_{s,i,t}\leqslant U_{i,t}^{\mathrm{GM}}\ \ \&\\ \quad D_i^{\mathrm{GQ}}(U_{i,t}^{\mathrm{GM}}-U_{s,i,t})\leqslant Q_i^{\mathrm{GM}}\\ 0, U_{i,t}^{\mathrm{GM}}<U_{s,i,t}<U_{i,t}^{\mathrm{AM}}\\ -D_i^{\mathrm{AQ}}(U_{s,i,t}-U_{i,t}^{\mathrm{AM}}), U_{s,i,t}\geq U_{i,t}^{\mathrm{AM}}\ \ \&\\ \quad D_i^{\mathrm{AQ}}(U_{s,i,t}-U_{i,t}^{\mathrm{AM}})\leqslant Q_i^{\mathrm{AM}}\\ -Q_i^{\mathrm{AM}}, D_i^{\mathrm{AQ}}(U_{s,i,t}-U_{i,t}^{\mathrm{AM}})>Q_i^{\mathrm{AM}}\end{cases}\quad ,i\in\boldsymbol{N}_{\mathrm{H}}\tag{5}$$

where $Q_{s,i,t}^{\mathrm{H}}$ is the reactive power injection of the hydrogen source; Q_i^{GM} and Q_i^{AM} are the maximum reactive power generation and absorption; U_i^{GM} and U_i^{AM} are the droop mode thresholds; D_i^{GQ} and D_i^{AQ} are the droop coefficients.

Noted that the piecewise Eqs. (3) to (5) can be used for both grid-forming and grid-following inverter-based hydrogen sources, but they are usually reversely formulated as $P-f$ and $Q-U$ functions in a grid-forming mode.

• Type 2: Electrical-chemical constraints

The intrinsic characteristics differentiating hydrogen sources from other traditional energy storage systems (e.g., batteries) lie in the power-to-hydrogen (P2H) and hydrogen-to-power (H2P) conversion process in electrolyzer and fuel cell, among which the nonlinear stack efficiency as a significant characteristic[4,5] is specifically modeled in this letter.

The following constraints describe the relationship of power output/input, hydrogen flow rate, and stack efficiency[4,5]:

$$\dot{m}_{s,i,t}^{\mathrm{He}}=\eta_{s,i,t}^{\mathrm{He}}P_{s,i,t}^{\mathrm{He}}, i\in\boldsymbol{N}_{\mathrm{H}}\tag{6}$$

$$P_{s,i,t}^{\mathrm{Hf}}=\dot{m}_{s,i,t}^{\mathrm{Hf}}\eta_{s,i,t}^{\mathrm{Hf}}, i\in\boldsymbol{N}_{\mathrm{H}}\tag{7}$$

where $\dot{m}_{s,i,t}^{\mathrm{He}}$ and $\dot{m}_{s,i,t}^{\mathrm{Hf}}$ are the hydrogen generation and consumption rates of the electrolyzer and fuel cell; $\eta_{s,i,t}^{\mathrm{He}}$ and $\eta_{s,i,t}^{\mathrm{Hf}}$ are the stack efficiencies, which are nonlinearly dependent on $P_{s,i,t}^{\mathrm{He}}$ and $P_{s,i,t}^{\mathrm{Hf}}$ [4, 5]. To linearize $\eta_i^{\mathrm{He}}(P_{s,i,t}^{\mathrm{He}})$ and $\eta_i^{\mathrm{Hf}}(P_{s,i,t}^{\mathrm{Hf}})$ and also the constraints of (6) and (7), the piecewise linearization method is adopted [8]:

$$\eta_{s,i,t}^{\mathrm{He/f}}=\begin{cases}\eta_i^{\mathrm{He/f}_{(1)}}, 0\leqslant P_{s,i,t}^{\mathrm{He/f}}\leqslant P_i^{\mathrm{He/f}_{(1)}}\\ \eta_i^{\mathrm{He/f}_{(2)}}, P_i^{\mathrm{He/f}_{(1)}}<P_{s,i,t}^{\mathrm{He/f}}\leqslant P_i^{\mathrm{He/f}_{(2)}}\\ \cdots\\ \eta_i^{\mathrm{He/f}_{(W)}}, P_i^{\mathrm{He/f}_{(W-1)}}<P_{s,i,t}^{\mathrm{He/f}}\leqslant P_i^{\mathrm{He/fM}}\end{cases}\quad ,i\in\boldsymbol{N}_{\mathrm{H}}\tag{8}$$

where $P_i^{\mathrm{He/f}_{(1)}}<P_i^{\mathrm{He/f}_{(2)}}<\cdots<P_i^{\mathrm{He/f}_{(W-1)}}$ are the linearization interval boundaries of the electrolyzer or fuel cell; W is the number of intervals; $\eta_i^{\mathrm{He/f}_{(w)}}$ is the constant stack efficiency at interval w, and can be approximated by:

$$\eta_i^{\mathrm{He/f}_{(w)}}=\frac{\eta_i^{\mathrm{He/f}}(P_{s,i,t}^{\mathrm{He/f}_{(w-1)}})+\eta_i^{\mathrm{He/f}}(P_{s,i,t}^{\mathrm{He/f}_{(w)}})}{2}\tag{9}$$

Besides the P2H and H2P constraints, the following hydrogen storage constraints[4] should also be incorporated:

$$m_{s,i,t}^{\mathrm{H}}=m_{s,i,t-1}^{\mathrm{H}}+x_{i,t}^{\mathrm{He}}\dot{m}_{s,i,t}^{\mathrm{He}}-x_{i,t}^{\mathrm{Hf}}\dot{m}_{s,i,t}^{\mathrm{Hf}}, i\in\boldsymbol{N}_{\mathrm{H}}\tag{10}$$

$$0\leqslant m_{s,i,t}^{\mathrm{H}}\leqslant m_i^{\mathrm{HM}}, i\in\boldsymbol{N}_{\mathrm{H}}\tag{11}$$

where $m_{s,i,t}^{\mathrm{H}}$ is the hydrogen mass; m_i^{HM} is the maximum hydrogen mass allowed for the storage; $x_{i,t}^{\mathrm{He}}$ and $x_{i,t}^{\mathrm{Hf}}$ are the binary variables to decide whether the electrolyzer or the fuel cell is working that should satisfy:

$$x_{i,t}^{\mathrm{He}}+x_{i,t}^{\mathrm{Hf}}\leqslant 1, i\in\boldsymbol{N}_{\mathrm{H}}\tag{12}$$

Regarding the secondary DERs, this letter takes the renewable sources as an example, since they are usually co-operated with hydrogen sources in microgrids[3]. The corresponding constraints can be found in Ref. [1]. To complete the optimization, the network and security constraints in Ref. [1] are also added.

The optimization model has several piecewise linear constraints like (3)–(5), and (8) and nonlinear product terms like (6), (7), and (10) which can be converted to linear constraints by using the big-M method. The converted model belongs to the mixed integer linear programming (MILP) and can be solved by commercial solvers like Gurobi, CPLEX, etc.

3 Case study

The proposed optimization model is validated on a modified IEEE 13 bus test feeder, where Buses 645 and 684 are integrated with two hydrogen sources to power the microgrid, and Buses 633 and 680 are integrated with two wind farms. The load weight is randomly selected from $(0,1)$ and those loads with a weight larger than 0.7 are regarded as critical loads. The optimization time window is set to 6 hours, and the 15-min interval forecast data for wind farms and loads are from the ENTSO-E Transparency Platform and are scaled down to fit the magnitude of this microgrid. The forecast errors of each wind power output and load demand are assumed to follow the normal distribution $N(0,10\%P^{\max})$. Two extreme scenarios with maximum and minimum average power and the original forecast scenario are used for the stochastic optimization. Their probabilities are set to 0.001, 0.001 and 0.998 so to maintain the economy and robustness of the optimized strategy.

(1) Model validation

The proposed optimization model with new hydrogen constraints is compared with the traditional model in Ref. [3]. The resilience indices (1) of the critical loads, non-critical loads and all loads for each time slot during the time window are calculated by the two models and shown in Figures 1(a) and 1(b).

Comparing Figures 1(a) and 1(b), it can be seen that the operation strategy by the proposed model brings the average LSR of critical loads from 100% down to 88.57% and the average LSR of non-critical loads from 8.98% up to 19.60% respectively. Nonetheless, the served critical loads are still far more than the served non-critical loads, and the average LSR of all loads is not significantly affected, indicating the effectiveness of the resilience-oriented model.

To further validate the two types of hydrogen constraints,

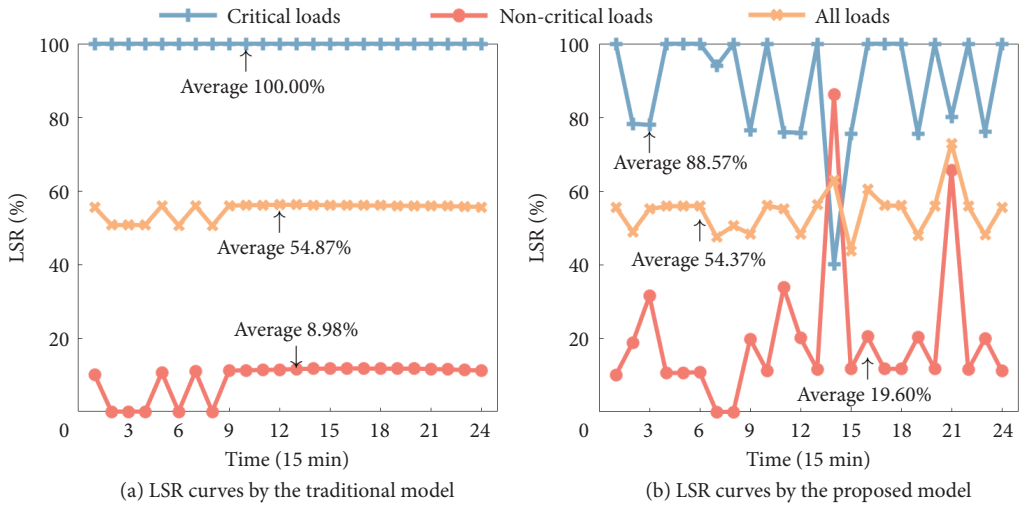

(a) LSR curves by the traditional model (b) LSR curves by the proposed model

Figure 1 LSR curves of different types of loads by the two models.

(3)–(5) and (6)–(12) are respectively replaced with the corresponding constraints in Ref. [3]. The maximum frequency and voltage variations of hydrogen sources with and without the regulation constraints are shown in Figure 2(a), and the states of hydrogen at the forecast scenario with and without the nonlinear stack efficiency constraints are shown in Figure 2(b).

As shown in Figure 2(a), the proposed model can drastically reduce the frequency and voltage variations and limit them in the allowable ranges (1 Hz and 100 V in this case study), while the operation strategy obtained by the traditional model without regulation constraints could easily lead to frequency and voltage violations and potential stability problems.

On the other hand, Figure 2(b) shows that the estimated states of hydrogen at specific scenario by the models with and without consideration of the nonlinear stack efficiency are remarkably different. The average absolute errors for hydrogen source 1 (between the two solid lines) and 2 (between the two dotted lines) are 4.09 kg and 4.26 kg. This might cause misestimations of hydrogen storage states within the operation time window, and even infeasibility of the resolution.

Thus, incorporating the frequency and voltage regulation constraints and the nonlinear stack efficiency related electrical-chemical conversion constraints proposed in this letter can help ensure the safety and security and improve the practicability and feasibility of the optimized microgrid operation plans.

(2) Resilience contribution of hydrogen sources

The resilience contribution of primary hydrogen sources comes from their capabilities of energy storage and frequency and voltage regulations. To verify the resilience contribution in energy storage, five cases numbered A-E are created with 0 to 100% initial hydrogen mass with a 25% increment. The states of total hydrogen mass in different time slots at the forecast scenario are shown in Figure 3(a), and the increase percentages of the energy supply and objective value between two adjacent cases are shown in Figure 3(b).

It can be seen from Figure 3(a) that, for Cases B, C, and D, the state of total hydrogen gradually decreases to zero in different rates (Cases B < Case C < Case D), where only the fuel cells work for almost all the time slots. For Case E with full initial hydrogen storage, the hydrogen cannot be completely consumed at the end of the optimization time window. For Case A with no initial hydrogen at all, however, the hydrogen sources, especially the electrolyzers, still actively participate in the energy management, and there is some amount of hydrogen mass accumulated in the end.

More interestingly, as shown in Figure 3(b), with increased initial hydrogen mass from Case A to E, the energy supply increases by around 6% for each pair of the cases. However, the objective value, which also indicates the system resilience, increases by significantly

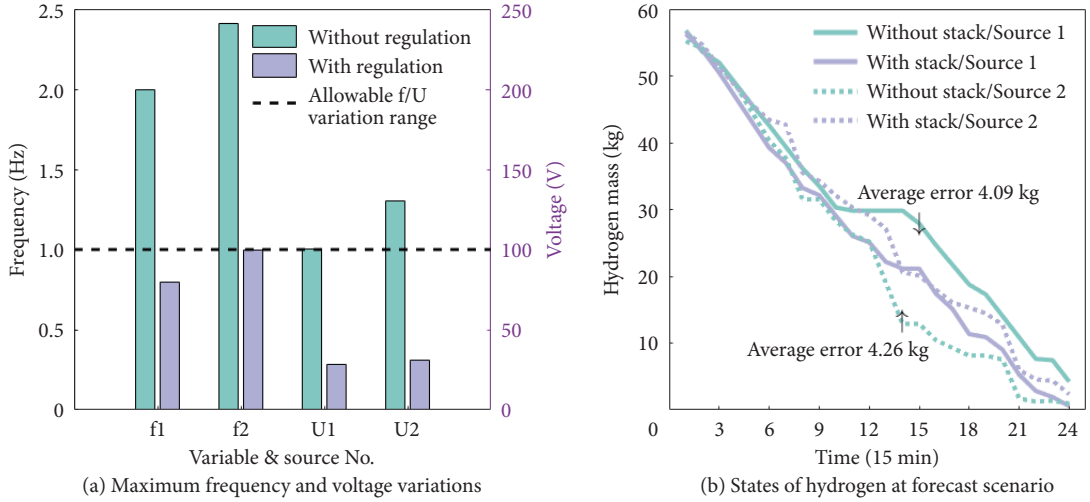

(a) Maximum frequency and voltage variations (b) States of hydrogen at forecast scenario

Figure 2 Optimization results with and without specific type of constraints.

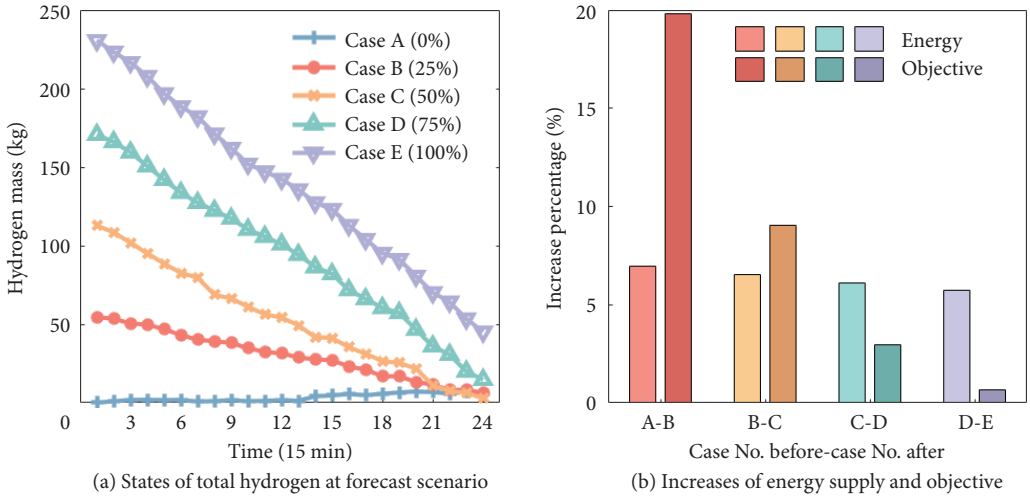

(a) States of total hydrogen at forecast scenario

(b) Increases of energy supply and objective

Figure 3 Optimization results of cases with different initial hydrogen masses.

different and monotonously decreasing percentages of about 20%, 9%, 3%, and 0.7%. This means that in this studied system, the hydrogen sources contribute the most marginal contribution to system resilience at a small or moderate initial hydrogen mass. The resilience cannot be notably increased by adding more hydrogen when the mass comes close to the storage limit.

To quantify another resilience contribution by priamry hydrogen sources in frequency and voltage regulations, three cases numbered I-III are created with different values of droop coefficients. The droop coefficients of Case I and Case II are four times and two times respectively those of Case III. Since the larger the droop coefficients are, the stronger the regulation capability is, the regulation capabilities of the hydrogen sources in these cases should be: Case I < Case II < Case III. Table 1 shows some operation indices in these cases.

Table 1 Operation Indices under Different Frequency and Voltage Regulation Capabilities of Hydrogen Sources

Index name	Case I	Case II	Case III
Objective value (1E7)	2.0735	2.9913	3.3121
Average LSR of all loads (%)	35.8815	49.2223	54.3692
Average LSR of critical loads (%)	56.0904	80.2319	88.5656
Renewable consumption ratio (%)	61.7913	86.9568	98.0403
Average frequency variation (Hz)	0.7269	0.6817	0.4684
Average voltage variation (V)	11.1005	10.9114	9.0844

It can be learned from Table 1 that, with increased capability of frequency and voltage regulations of the primary hydrogen sources, the objective value, the LSR of all loads, the LSR of critical loads, and the renewable consumption ratio are all improved drastically, by 59.73%, 51.52%, 57.90% and 58.66% respectively. Thus, two straightforward benefits of enhancing the regulation capability of hydrogen sources are that more critical loads can be served and that more intermittent renewable energy can be consumed.

Meanwhile, it can be seen from the last two lines of Table 1 that both the frequency and voltage variations show a prominent decreasing trend, which are reduced by 35.56% and 18.16% respectively. This indicates another important benefit of primary hydrogen sources that they can reduce the frequency and voltage fluctuations caused by uncertainties and disturbances to a great extent, thus effectively enhancing system security and also resilience.

4 Conclusions

This letter proposes an operational optimization formulation for hydrogen-powered microgrids, that incorporates the constraints of frequency and voltage regulations and electrical-chemical conversion process of primary hydrogen sources.

Test results show that the proposed concept has the following potential practical merits: (1) It can generate a more realistic and practicable microgrid operation plan than the traditional model; (2) It can ensure a high resilience under blackouts by serving as many critical loads as possible; (3) It can reduce the frequency and voltage variations and limit them in allowable ranges to guarantee system security under disturbances; 4) It can increase the renewable energy utilization rate and thus help reduce the carbon emission.

Despite the promising technical merits, the hydrogen and the associated infrastructure are now still too costly. Rather, this letter lays a solid theoretical foundation for resilient operation of hydrogen-powered microgrids, that can be hopefully used for small-scale demonstrative projects in the near future.

Acknowledgements

This work relates to the U.S. Department of Navy award N00014-23-1-2124 issued by the Office of Naval Research. The United States Government has a royalty-free license throughout the world in all copyrightable material contained herein.

Article history

Received: 11 June 2024; Revised: 26 June 2024; Accepted: 28 June 2024

Additional information

Declaration of competing interest

The authors have no competing interests to declare that are relevant to the content of this article.

References

[1] Lin, C., Chen, C., Liu, F., Li, G., Bie, Z.. (2022). Dynamic MGs-based load restoration for resilient urban power distribution systems considering intermittent RESs and droop control. *International Journal of Electrical Power & Energy Systems*, 140: 107975.

[2] U.S. Department of Energy (2020). Department of energy hydrogen program plan. Available at https://www.hydrogen.energy.gov/docs/hydrogenprogramlibraries/pdfs/hydrogen-program-plan-2020.pdf

[3] Zhao, Y., Lin, J., Song, Y., Xu, Y.. (2023). A hierarchical strategy for restorative self-healing of hydrogen-penetrated distribution systems considering energy sharing via mobile resources. *IEEE Transactions on Power Systems*, 38: 1388–1404.

[4] De Corato, A. M., Ghazavi Dozein, M., Riaz, S., Mancarella, P.. (2023). Hydrogen electrolyzer load modelling for steady-state power system studies. *IEEE Transactions on Power Delivery*, 38: 4312–4323.

[5] Chiara Massaro, M., Pramotton, S., Marocco, P., Monteverde, A. H. A., Santarelli, M.. (2024). Optimal design of a hydrogen-powered fuel cell system for aircraft applications. *Energy Conversion and Management*, 306: 118266.

[6] Bie, Z., Bian, Y. (2024). Microgrids resilience: Definition, measures, and algorithms. In: Zhang, P. Ed. *Microgrids: Theory and Practice*. Hoboken, NJ, USA: John Wiley & Sons.

[7] IEEE Standards Coordinating Committee 21 (2018). IEEE Standard for Interconnection and Interoperability of Distributed Energy Resources with Associated Electric Power Systems Interfaces. Available at https://ieeexplore.ieee.org/document/8365917.

[8] Wang, J., He, G., Song, J. (2024). Hydrogen-supported microgrid toward lowcarbon energy transition. In: Zhang, P. Ed. *Microgrids: Theory and Practice*. Hoboken, NJ, USA: John Wiley & Sons.